

# Can the edges of a complete graph form a radially symmetric field in closed space of constant positive curvature?

S. Halayka\*

July 25, 2010

## Abstract

In earlier work, it was found that the edges of a complete graph can very nearly form a radially symmetric field at long distance in flat 2D and 3D space if the number of graph vertices is great enough. In this work, it is confirmed that the edges of a complete graph can also very nearly form a radially symmetric field in closed 2D and 3D space of constant positive curvature if the graph is small compared to the entirety of the space in which it lives and if the number of graph vertices is great enough.

## 1 Introduction

Complete graphs have been used to construct models of quantum gravity [1–4].

It is considered here that a complete graph  $G_1$  living in closed  $dD$  space of constant positive curvature consists of:

1.  $n(G_1)$  vertices  $V(G_1)$  that are uniformly distributed along a  $(d-1)D$  shell  $S(G_1)$  of colatitude  $\Phi(G_1) = (0, \pi)$ .
2.  $(n(G_1)^2 - n(G_1))/2$  edges  $E(G_1)$  (e.g., great circles) that join the unique vertex pairs together.

See Figure 1 for a complete graph in flat 2D space, and Figure 2 for a complete graph in closed 2D space of constant positive curvature.

It seems fundamentally important to question whether or not the graph edges can form a radially symmetric field at long distance.

## 2 Method

If the field is to be considered radially symmetric, then the following two fitness criteria must be met:

---

\*shalayka@gmail.com

1. With regard to a second  $(d - 1)$ D shell  $S(G_2)$  of differing colatitude  $\Phi(G_2) \neq \Phi(G_1)$ , the  $n(G_2)$  vertices  $V(G_2)$  corresponding to where the graph edges  $E(G_1)$  intersect with  $S(G_2)$  should be uniformly distributed along  $S(G_2)$ .
2. With regard to each intersection vertex, the corresponding edge direction vector  $\widehat{E}_{dir}(G_1)$  should be identical to the corresponding longitudinal tangent vector  $\widehat{V}_{lt}(G_2)$  on  $S(G_2)$ .

In the earlier work on flat space [5, 6], the number of intersection vertices was defined to be  $n(G_2) \equiv n(G_1)^2 - n(G_1)$ . However, in this work [7] the number of intersection vertices per edge can be anywhere from zero to two depending on the edge's rotational orientation with respect to  $S(G_2)$ , and so  $n(G_2) = [0, n(G_1)^2 - n(G_1)]$ .

With regard to the first criterion (e.g., uniform distribution fitness), the vertices  $V(G_2)$  will be compared to  $n(G_3) \equiv n(G_1)^2 - n(G_1)$  vertices  $V(G_3)$  that are known to be uniformly distributed along a third and final  $(d - 1)$ D shell  $S(G_3)$  of colatitude  $\Phi(G_3) = \Phi(G_2)$ .

The uniform distribution fitness test used here compares  $n(G_3)$  pairs of vertices  $V(G_2)_i, V(G_3)_i$  by first constructing a pair of flat space complete graphs out of  $V(G_2), V(G_3)$ , and then analyzing the lengths of the internal portions of their corresponding edges  $I(V(G_2)_i)_j, I(V(G_3)_i)_j$  (e.g., where  $i = \{1, 2, \dots, n(G_3)\}, j = \{1, 2, \dots, n(G_3) - 1\}$ ). It is important to note that since  $V(G_2)$  may be less than  $V(G_3)$ , it is possible that the vertex/edge referred to by  $I(V(G_2)_i)_j$  is actually non-existent. In this event, a length value of 0 is used by default.

Some kind of order must be established so that a reasonable correlation exists between  $I(V(G_2)_i)_j, I(V(G_3)_i)_j$ , and so the lengths are placed into a pair of sorted bins before the comparison begins

$$L(I(V(G_2)_i)) = \text{sort}[\text{length}[I(V(G_2)_i)_1], \dots, \text{length}[I(V(G_2)_i)_{(n(G_3)-1)}]], \quad (1)$$

$$L(I(V(G_3)_i)) = \text{sort}[\text{length}[I(V(G_3)_i)_1], \dots, \text{length}[I(V(G_3)_i)_{(n(G_3)-1)}]]. \quad (2)$$

Since non-existent vertex/edge length values are 0 by default, it is guaranteed that the sorted bin  $L(I(V(G_2)_i))$  exists, and that its number of elements is equal to  $n(G_3) - 1$  regardless of the value of  $n(G_2)$ . For instance where  $n(G_2) = 0$ , all  $n(G_3)$  sorted bins  $L(I(V(G_2)_i))$  would contain  $n(G_3) - 1$  elements with the value of 0 (e.g., all zeroes).

Ideally, since  $V(G_3)$  are known to be uniformly distributed along  $S(G_3)$ , the  $n(G_3)$  sorted bins  $L(I(V(G_3)_i))$  should all contain identical length distributions (e.g., thus defining a single reference distribution  $L(I(V(G_3)))_{\text{ref}}$ ). Likewise, if  $n(G_2) = n(G_3)$  and  $V(G_2)$  are also uniformly distributed along  $S(G_2)$ , then the  $n(G_2) = n(G_3)$  sorted bins  $L(I(V(G_2)_i))$  should also all contain length distributions that are identical to  $L(I(V(G_3)))_{\text{ref}}$ .

The uniform distribution fitness test used here is

$$F_D(G_1, G_2) = \frac{\sum_{i=1}^{n(G_3)} \sum_{j=1}^{(n(G_3)-1)} \frac{\min[L(I(V(G_2)_i))_j, L(I(V(G_3)_i))_j]}{\max[L(I(V(G_2)_i))_j, L(I(V(G_3)_i))_j]}}{n(G_3)^2 - n(G_3)}. \quad (3)$$

It is useful to note that each edge's internal portion is analyzed exactly twice throughout the entire test, which is why equation (3) is normalized using  $n(G_3)^2 - n(G_3)$ , not  $(n(G_3)^2 - n(G_3))/2$ .

With regard to the second criterion (e.g., tangent fitness), the test used here is

$$F_T(G_1, G_2) = \frac{\sum_{k=1}^{n(G_2)} \hat{E}_{dir}(G_1)_k \cdot \hat{V}_{lt}(G_2)_k}{n(G_3)}. \quad (4)$$

It is useful to note that equation (4) is normalized using the maximum possible number of intersection vertices  $n(G_3)$ , not the actual number of intersection vertices  $n(G_2)$ . This provides for a more stringent test, as well as protection against a divide by zero operation where  $n(G_2) = 0$ .

### 3 Results

Figure 3 shows a complete graph living in closed 2D space of constant positive curvature. Because the graph colatitude is  $\Phi(G_1) \sim 0.5\pi$ , the graph edges run mostly East-West (e.g., not North-South). Since the test shell colatitude  $\Phi(G_2) = 0.33\pi$  is much different than the graph colatitude, the result is fitness test values of  $F_D(G_1, G_2) = 0$ ,  $F_T(G_1, G_2) = 0$ . The edges fail to form any kind of field at the test shell, let alone a radially symmetric one. However, as shown in Figure 4, a sufficient increase in  $n(G_1)$  alone can form a field that results in non-zero fitness test values (e.g.,  $F_D(G_1, G_2) \approx 0.002$ ,  $F_T(G_1, G_2) \approx 0.02$ ).

For the sake of reference, Figure 5 shows a polar azimuthal projection of a complete graph living in closed 2D space of constant positive curvature, where  $\Phi(G_1) = 0.8\pi$ ,  $\Phi(G_2) = 0.4\pi$ ,  $F_D(G_1, G_2) \approx 0.94$ ,  $F_T(G_1, G_2) \approx 0.91$ . To compare, Figure 6 shows a polar azimuthal projection of a complete graph living in closed 3D space of constant positive curvature, where  $\Phi(G_1) = 0.95\pi$ ,  $\Phi(G_2) = 0.19\pi$ ,  $F_D(G_1, G_2) \approx 0.94$ ,  $F_T(G_1, G_2) \approx 0.99$ .

Figure 7 shows a complete graph living in closed 3D space of constant positive curvature. Because the graph colatitude  $\Phi(G_1) = 0.7\pi$  is relatively close to  $0.5\pi$ , all but one of the edges run mostly East-West-Up-Down (e.g., not North-South). The test shell colatitude is  $\Phi(G_2) = 0.19\pi$ , and the result is fitness test values of  $F_D(G_1, G_2) \approx 0.005$ ,  $F_T(G_1, G_2) \approx 0.1$ .

Although not shown here, a graph colatitude of  $\Phi(G_1) = 0$  or  $\Phi(G_1) = \pi$  would signify a classical point-like object (e.g., no graph interior). In this case, the edges are *a priori* taken to run purely North-South in an evenly distributed fashion, regardless of the dimension  $d$  of the closed space in which the graph

lives. This classical edge configuration always results in fitness test values of 1, regardless of test shell colatitude. This configuration also forms edge singularities (e.g., caustics) at both the North and South poles, regardless of which pole the graph shell is actually closest to.

## 4 Discussion

According to results presented here, the edges of a complete graph can very nearly form a radially symmetric field in closed 2D and 3D space of constant positive curvature if the graph is small compared to the entirety of the space in which it lives (e.g.,  $\Phi(G_1) \ll 0.5\pi$  or  $\Phi(G_1) \gg 0.5\pi$ ) and if the number of graph vertices is great enough (e.g.,  $n \gg 1$ ).

The relevance of these results depends on at least the following two lines of questions:

1. Have equatorial-sized black holes (e.g.,  $\Phi(G_1) \sim 0.5\pi$ , see Figures 3, 4) existed in the past? If complete graphs are used to model equatorial-sized black holes, are the resulting very low fitness test values at long distance catastrophically detrimental to the formation of the presently observed Universe (e.g., would stars still form)? If equatorial-sized complete graph black holes are not catastrophically detrimental, and perhaps existed in the past, then do they still exist today? If so:
  - Would the mass-energy of equatorial-sized black holes somehow relate to the theoretical discrepancy between the Planck scale and the cosmological constant scale (e.g., the cosmological constant problem)?
  - Would the accelerating evaporation of equatorial-sized black holes over time via Hawking radiation somehow relate to the presently observed accelerating expansion of space (e.g., the dark energy problem)?
2. Do much-greater-than-equatorial-sized complete graph black holes (e.g.,  $\Phi(G_1) \sim \pi$ , see Figure 6) exist today? For instance, if mass-energy is added to an equatorial-sized black hole, it seems inevitable that the event horizon area would shrink. Beyond  $\Phi(G_1) = 0.5\pi$ , the black hole's entropy would become too great for its event horizon area, seemingly breaking the Bekenstein entropy bound. However, it seems more likely that as the event horizon colatitude increases beyond  $\Phi(G_1) = 0.5\pi$ , the black hole's interior and exterior regions would effectively swap places (e.g., the black hole would flip inside-out), and that the black hole's "too-great" entropy would relate not to the black hole's interior region anymore, but to its exterior region. If so:
  - Would much-greater-than-equatorial-sized black holes somehow relate to the presently observed set of fundamental particles? For instance, is the apparent mass-energy of a fundamental particle some-

how only a tiny fraction of the particle's actual mass-energy (e.g., the tip of the iceberg, so to speak)? If so:

- Would much-greater-than-equatorial-sized black holes somehow relate to the cosmological constant and dark energy problems?

See [7] for the public domain fitness test C++ code. Because no vector cross product operations were used in the code, it is inherently dimension-independent. The code includes the Mersenne Twister pseudorandom number generator code [8]. The accompanying OpenGL 1.x code (used to generate the figures given here) includes the following code:

- Direction vector to OpenGL yaw-pitch angle conversion code from JYK.
- NeHe Productions - OpenGL Lesson #37 [9].
- OpenGL @ Lighthouse 3D - GLUT Tutorial (Bitmap Fonts and Orthogonal Projections) [10].

Dedicated to: GV, JYK, P, A, C, Shark, J, Honey Dog.

## References

- [1] Antonsen F. Random graphs as a model for pregeometry. (1994) Int J Theor Phys 33: 1189-1205
- [2] Gibbs PE. The Small Scale Structure of Space-Time: A Bibliographical Review. (1995) arXiv:hep-th/9506171v2
- [3] Konopka T, Markopoulou F, Smolin L. Quantum Graphity. (2006) arxiv:hep-th/0611197
- [4] Konopka T, Markopoulou F, Severini S. Quantum Graphity: a model of emergent locality. (2008) arXiv:0801.0861v2 [hep-th]
- [5] Halayka S. Can the External Directed Edges of a Complete Graph Form a Radially Symmetric Field at Long Distance? (2010) viXra:1003.0275
- [6] Halayka S. Flat space fitness test C++ code v3.0. (2010) [http://completegraph-rays.googlecode.com/files/rays\\_3.0.zip](http://completegraph-rays.googlecode.com/files/rays_3.0.zip)
- [7] Halayka S. Closed space fitness test C++ code v1.1. (2010) <http://code.google.com/p/completegraphcurved/downloads/list>
- [8] Saito M, Matsumoto M, Hiroshima University. SIMD-oriented Fast Mersenne Twister ("SFMT") v1.3.3. (2006) <http://www.math.sci.hiroshima-u.ac.jp/~m-mat/MT/SFMT/>
- [9] Hamlaoui S. NeHe Productions - OpenGL Lesson #37. (2002) <http://nehe.gamedev.net/data/lessons/lesson.asp?lesson=37>

- [10] Ramires Fernandes A. OpenGL @ Lighthouse 3D - GLUT Tutorial (Bitmap Fonts and Orthogonal Projections). (2005) <http://www.lighthouse3d.com/opengl/glut/index.php?bmpfontortho>

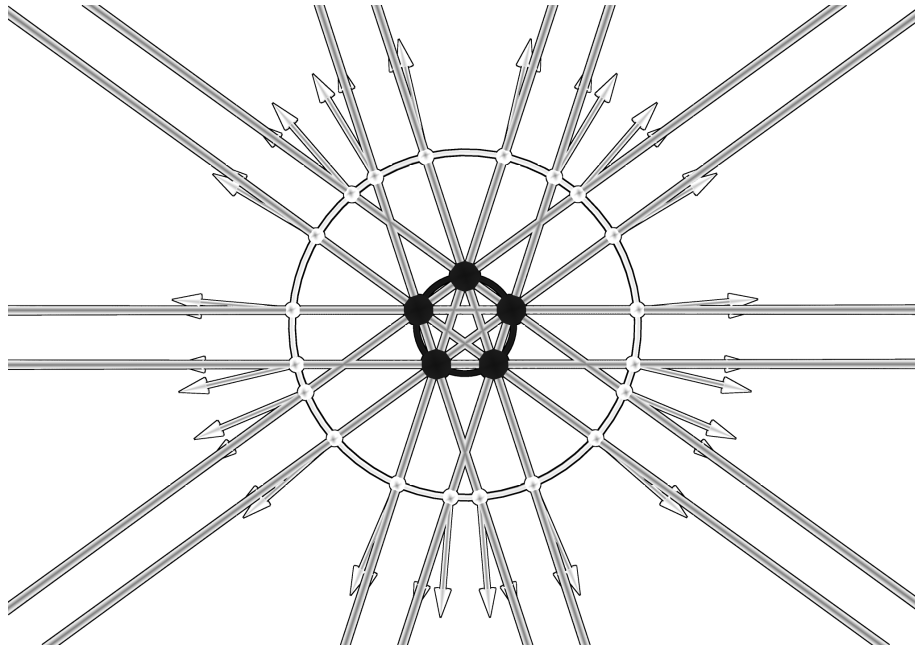


Figure 1: A complete graph  $G_1$  (e.g.,  $n(G_1) = 5$  black vertices along a black 1D shell  $S(G_1)$ , plus  $(n(G_1)^2 - n(G_1))/2$  gray straight edges) in approximately flat 2D space. The test object  $S(G_2)$  (e.g., a second 1D shell, light gray in this case) has a radius  $r(G_2)$  that is roughly three times greater than the graph radius  $r(G_1)$ . Uniform distribution fitness is  $F_D(G_1, G_2) \approx 0.94$ , normal fitness is  $F_N(G_1, G_2) \approx 0.98$ .

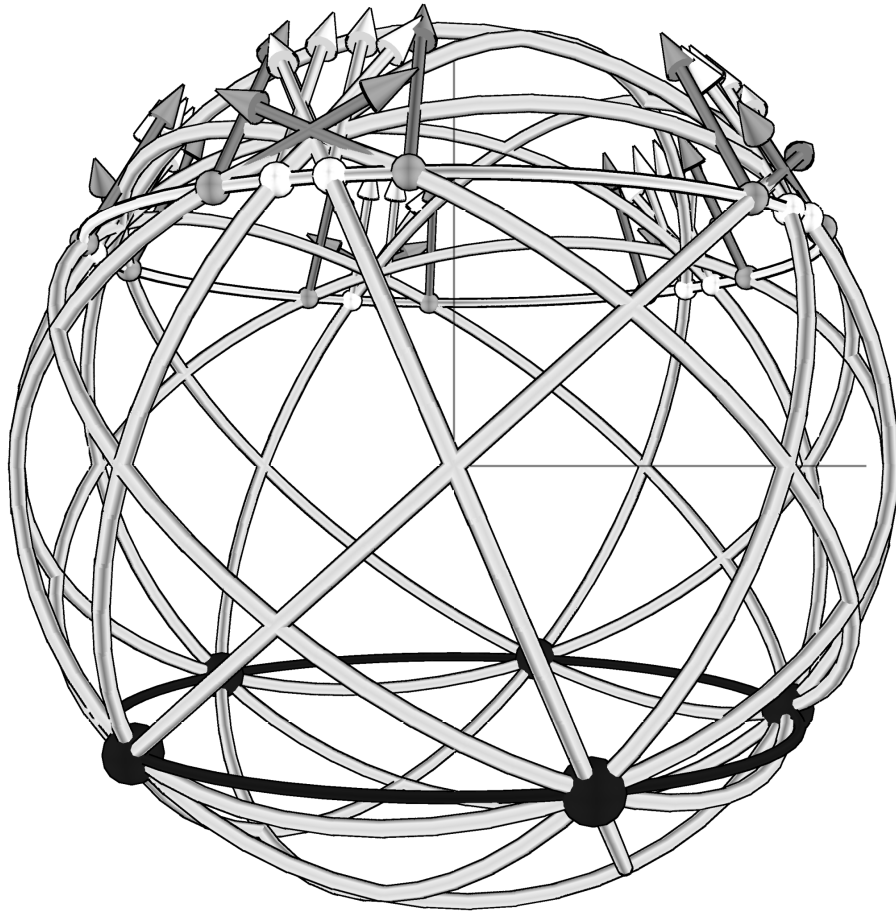


Figure 2: A complete graph in closed 2D space of constant positive curvature, where  $n(G_1) = 5$ . The graph edges are great circles in 3D space. Graph colatitude is  $\Phi(G_1) = 0.7\pi$  radians, test shell colatitude is  $\Phi(G_2) = 0.33\pi$  radians. Uniform distribution fitness is  $F_D(G_1, G_2) \approx 0.89$ , tangent fitness is  $F_T(G_1, G_2) \approx 0.7$ .



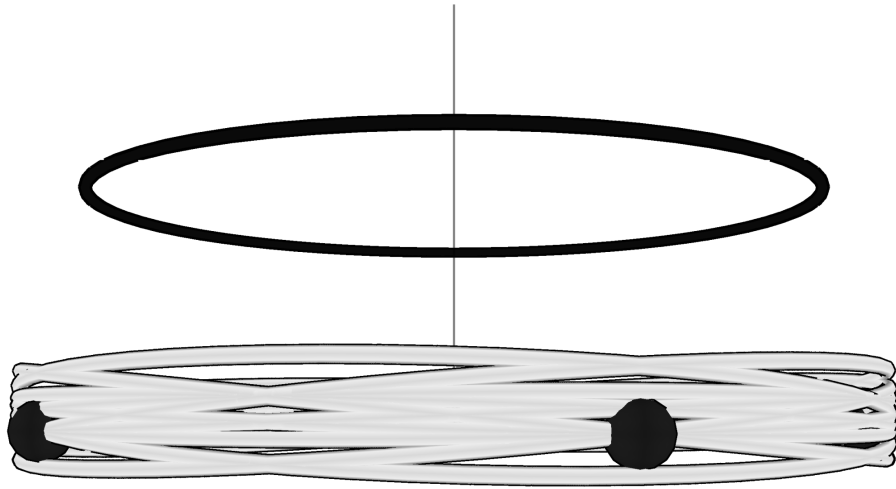


Figure 3: A complete graph in closed 2D space of constant positive curvature, where  $n(G_1) = 5$ .  $\Phi(G_1) = 0.51\pi$ ,  $\Phi(G_2) = 0.33\pi$ ,  $F_D(G_1, G_2) = 0$ ,  $F_T(G_1, G_2) = 0$  (e.g., the graph edges run mostly East-West).

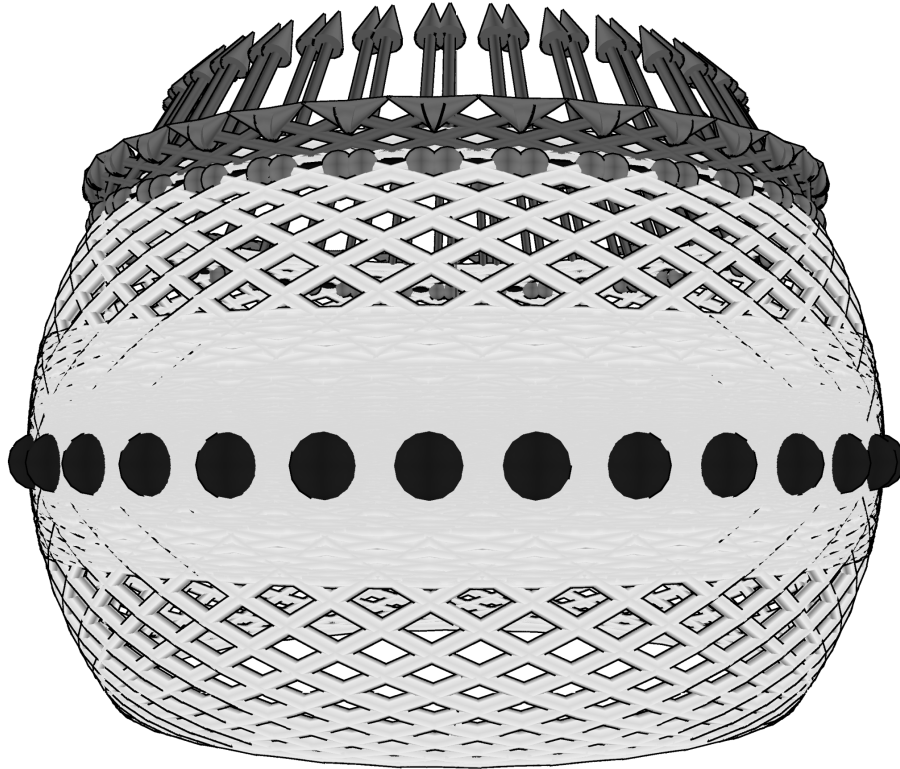


Figure 4: A complete graph in closed 2D space of constant positive curvature, where  $n(G_1) = 35$ .  $\Phi(G_1) = 0.51\pi$ ,  $\Phi(G_2) = 0.33\pi$ ,  $F_D(G_1, G_2) \approx 0.002$ ,  $F_T(G_1, G_2) \approx 0.02$ . The fitness test values are non-zero due to the relatively large value of  $n(G_1)$  (e.g. see Fig. 3 where  $n(G_1) = 5$ ).

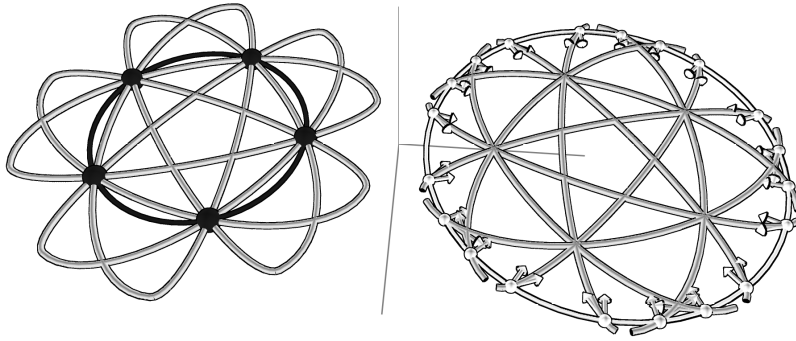


Figure 5: A complete graph in closed 2D space of constant positive curvature, where  $n(G_1) = 5$ . The graph edges are great circles in 3D space. The entire set of 3D objects has been projected onto flat 2D space via polar azimuthal projection (e.g., bisection along the equator, suppression of the third dimension). This causes the test shell 3D longitudinal tangent vectors to look like shortened test shell 2D normal vectors.  $\Phi(G_1) = 0.8\pi$ ,  $\Phi(G_2) = 0.4\pi$ ,  $F_D(G_1, G_2) \approx 0.94$ ,  $F_T(G_1, G_2) \approx 0.91$ .

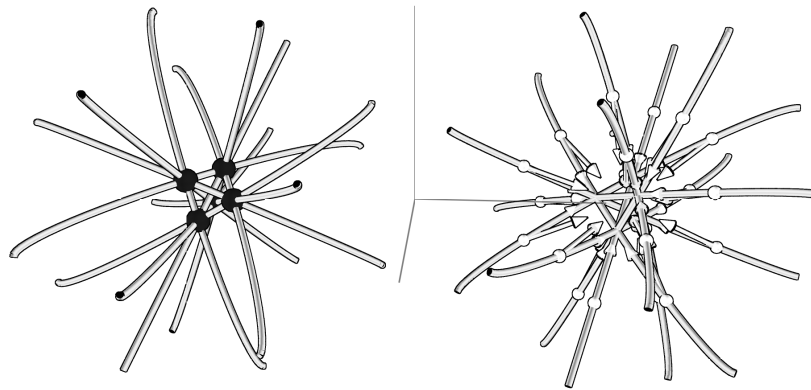


Figure 6: A complete graph in closed 3D space of constant positive curvature, where  $n(G_1) = 5$ . The graph edges are great circles in 4D space. The entire set of 4D objects has been projected onto flat 3D space via polar azimuthal projection (e.g., bisection along the equator, suppression of the fourth dimension). This causes the test shell 4D longitudinal tangent vectors to look like shortened test shell 3D normal vectors.  $\Phi(G_1) = 0.95\pi$ ,  $\Phi(G_2) = 0.19\pi$ ,  $F_D(G_1, G_2) \approx 0.94$ ,  $F_T(G_1, G_2) \approx 0.99$ .

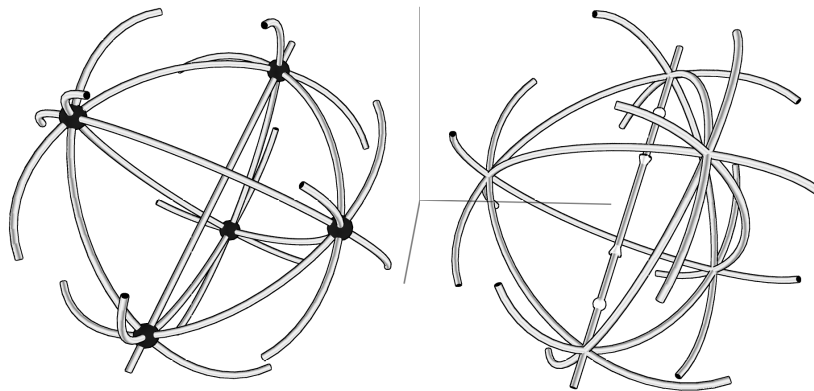


Figure 7: A complete graph in closed 3D space of constant positive curvature, where  $n(G_1) = 5$ .  $\Phi(G_1) = 0.7\pi$ ,  $\Phi(G_2) = 0.19\pi$ ,  $F_D(G_1, G_2) \approx 0.005$ ,  $F_T(G_1, G_2) \approx 0.1$  (e.g., only one graph edge runs mostly North-South, the rest run mostly East-West-Up-Down).